



# A pan-cancer analysis implicates human *NKIRAS1* as a tumor-suppressor gene

Thomas S. Postler<sup>a,1,2</sup> , Anqi Wang<sup>b,c,2</sup> , Francesco G. Brundu<sup>b,c</sup> , Pingzhang Wang<sup>b,c</sup>, Zikai Wu<sup>b,c</sup>, Kelly E. Butler<sup>a</sup> , Yenkel Grinberg-Bleyer<sup>a</sup> , Suneeta Krishnareddy<sup>a,d</sup>, Stephen M. Lagana<sup>e</sup>, Anjali Saqi<sup>e</sup> , Andrea Oeckinghaus<sup>a</sup> , Raul Rabadan<sup>b,c,3</sup> , and Sankar Ghosh<sup>a,3</sup>

Contributed by Sankar Ghosh; received July 25, 2023; accepted September 25, 2023; reviewed by Yinon Ben-Neriah and Jorge Moscat

The NF- $\kappa$ B family of transcription factors and the Ras family of small GTPases are important mediators of proproliferative signaling that drives tumorigenesis and carcinogenesis. The  $\kappa$ B-Ras proteins were previously shown to inhibit both NF- $\kappa$ B and Ras activation through independent mechanisms, implicating them as tumor suppressors with potentially broad relevance to human cancers. In this study, we have used two mouse models to establish the relevance of the  $\kappa$ B-Ras proteins for tumorigenesis. Additionally, we have utilized a pan-cancer bioinformatics analysis to explore the role of the  $\kappa$ B-Ras proteins in human cancers. Surprisingly, we find that the genes encoding  $\kappa$ B-Ras 1 (*NKIRAS1*) and  $\kappa$ B-Ras 2 (*NKIRAS2*) are rarely down-regulated in tumor samples with oncogenic Ras mutations. Reduced expression of human *NKIRAS1* alone is associated with worse prognosis in at least four cancer types and linked to a network of genes implicated in tumorigenesis. Our findings provide direct evidence that loss of *NKIRAS1* in human tumors that do not carry oncogenic *RAS* mutations is associated with worse clinical outcomes.

cancer | NF-kappaB | Ras proteins | NKIRAS | inflammation

At its most basic level, cancer can be viewed as a disease of aberrant signaling. Genomic changes resulting in the inappropriate activation of oncogene products and the loss of tumor-suppressor function, often augmented by proproliferative and antiapoptotic extrinsic factors caused by chronic inflammation, create a complex combination of signals that permit incipient tumor cells to proliferate in an uncontrolled fashion. Similar changes often allow tumor cells to escape anoikis and develop metastases during carcinogenesis. While all cancer types are uniquely different from each other, the advent of high-throughput genomics and transcriptomics has helped reveal certain mechanisms that apply to several cancers. Consequently, the so-called pan-cancer studies, which integrate sequencing and patient data across a large number of cancer types, have the potential to identify common drivers of tumorigenesis and carcinogenesis, as well as expand our knowledge of known tumor-promoting mechanisms to a broad range of tissues.

The Ras family of small GTPases and the NF- $\kappa$ B family of transcription factors are signaling regulators that have been widely implicated in promoting tumorigenesis. Indeed, *RAS* genes are generally believed to be mutated in approximately a fifth of all human cancers, placing them among the most frequently mutated oncogenes (1, 2). The human Ras proteins, K-Ras, H-Ras, and N-Ras, activate proproliferative signaling pathways primarily through their downstream effectors Raf, PI3K, and Ral. Of those, Ral signaling is particularly relevant for anchorage-independent proliferation (AIP), which is a hallmark of carcinogenesis and a requirement for metastasization (3). The transcription factors of the NF- $\kappa$ B family have also been implicated as major contributors to carcinogenesis, as they drive the expression of a range of antiapoptotic and proproliferative proteins (4). Unlike the *RAS* genes, however, the genes encoding NF- $\kappa$ B proteins are mutated exceedingly rarely in most human cancers. Instead, this pathway is frequently activated extrinsically in inflammation-driven cancers, by cytokines secreted into the tumor microenvironment by immune and other bystander cells. This proinflammatory environment can result from unrelated chronic inflammation, e.g., Crohn's disease or ulcerative colitis, or be induced by the incipient tumor itself. The activation of NF- $\kappa$ B signaling by these cytokines promotes proliferation and survival of tumor cells, allowing the tumor to grow and accumulate further mutations (5).

The  $\kappa$ B-Ras proteins,  $\kappa$ B-Ras 1 and 2, are highly conserved, atypical members of the Ras superfamily (6, 7). Their GTPase domain is catalytically inactive; hence, unlike other members of the Ras family, they do not use hydrolysis of bound GTP as a molecular switch to determine their activation state. Instead, we and others have shown that the  $\kappa$ B-Ras proteins serve to inhibit NF- $\kappa$ B activation by binding to and stabilizing the inhibitory protein I $\kappa$ B- $\beta$  (6, 8–11). This prevents excessive expression of several potent cytokines, in

## Significance

$\kappa$ B-Ras proteins inhibit two signaling pathways known to be important for carcinogenesis: NF- $\kappa$ B, a key regulator of inflammation, and Ral, a Ras effector protein important for metastasization. Here, we demonstrate that  $\kappa$ B-Ras deficiency promotes carcinogenesis in murine models of lung and colon cancer. A pan-cancer analysis reveals that in humans the coincidence of Ras mutation and reduced  $\kappa$ B-Ras expression is exceedingly rare, as is the co-occurrence of simultaneous reduction of  $\kappa$ B-Ras 1 and  $\kappa$ B-Ras 2. Instead, reduced  $\kappa$ B-Ras 1 expression, but not reduced  $\kappa$ B-Ras 2 expression, is associated with worse prognosis in several human cancers. This is particularly noteworthy because  $\kappa$ B-Ras 1 and  $\kappa$ B-Ras 2 are redundant in murine models, which does not appear to be the case in humans.

Author contributions: T.S.P., R.R., and S.G. designed research; T.S.P., A.W., F.G.B., P.W., K.E.B., Y.G.-B., S.K., and A.O. performed research; T.S.P., A.W., F.G.B., P.W., Z.W., Y.G.-B., S.M.L., A.S., A.O., R.R., and S.G. analyzed data; and T.S.P., R.R., and S.G. wrote the paper.

Reviewers: Y.B.-N., Universidad Hebraica; and J.M., Weill Cornell Medicine.

The authors declare no competing interest.

Copyright © 2023 the Author(s). Published by PNAS. This article is distributed under [Creative Commons Attribution-NonCommercial-NoDerivatives License 4.0 \(CC BY-NC-ND\)](https://creativecommons.org/licenses/by-nc-nd/4.0/).

<sup>1</sup>Present address: Vaccine Design and Development Laboratory, International AIDS Vaccine Initiative, New York, NY 11220.

<sup>2</sup>T.S.P. and A.W. contributed equally to this work.

<sup>3</sup>To whom correspondence may be addressed. Email: rr2579@cumc.columbia.edu or sg2715@columbia.edu.

This article contains supporting information online at <https://www.pnas.org/lookup/suppl/doi:10.1073/pnas.2312595120/-/DCSupplemental>.

Published November 6, 2023.

particular Tnf. More recently, we reported that the  $\kappa$ B-Ras proteins fulfill a second, independent role as inhibitors of Ral signaling. Specifically,  $\kappa$ B-Ras proteins bind to the Ral GTPase-activating protein (RalGAP) complex and enhance its activity, thus inhibiting Ral activity. Consistent with this, deletion of both  $\kappa$ B-Ras-encoding genes in immortalized cell lines promotes their ability for AIP (12). Moreover, the increased activation of Ral signaling that results from loss of the  $\kappa$ B-Ras proteins accelerates mortality in a K-Ras-driven mouse model of pancreatic ductal adenocarcinoma (PDAC), by promoting acinar-to-ductal metaplasia (13). Therefore,  $\kappa$ B-Ras proteins are likely to function as unique tumor suppressors by inhibiting inflammation-driven and Ras-driven oncogenesis through independent molecular mechanisms.

While several studies have reported that the expression of  $\kappa$ B-Ras proteins is significantly reduced in a variety of human cancers, the physiological relevance of this observation remains to be fully explored (12–22). Here, we demonstrate that  $\kappa$ B-Ras deficiency promotes carcinogenesis in murine models of Ras-driven lung and colon cancer. Moreover, to more deeply explore the role of  $\kappa$ B-Ras proteins in human tumors, we have carried out a pan-cancer analysis of the genes encoding  $\kappa$ B-Ras 1 and 2 (*NKIRAS1* and *NKIRAS2*). Surprisingly, we find that unlike in mice, *NKIRAS1* and *NKIRAS2* appear to have nonredundant roles in human tumors, with loss of *NKIRAS1* alone, even in the absence of *RAS* mutations, exhibiting a clear association with worse patient outcome in four highly disparate cancer types. These results establish a wider role of  $\kappa$ B-Ras 1 as a tumor suppressor than previously appreciated and reveal important differences between the murine and human *NKIRAS* orthologs.

## Results

**Two Mouse Models of Cancer Confirm the Tumor-Suppressive Properties of the  $\kappa$ B-Ras Proteins In Vivo.** We began our investigation by determining whether loss of the  $\kappa$ B-Ras proteins increases disease burden in two unrelated mouse models of cancer. To account for the dual role of  $\kappa$ B-Ras proteins as inhibitors of Ral signaling downstream of Ras activation and of NF- $\kappa$ B activation under proinflammatory conditions, we selected the mutant K-Ras<sup>G12D</sup>-driven model of lung cancer and the azoxymethane (AOM)/dextran sulfate sodium (DSS) model of inflammation-driven colon cancer. Unlike in human colorectal cancer, which is associated with a very high rate of oncogenic *KRAS* mutations, the AOM/DSS model only rarely exhibits *Kras* mutations (23–25). For the lung cancer model, we crossed our *Nkiras* conditional double-knock-out (cDKO) mice (*Nkiras1*<sup>-/-</sup> *Nkiras2*<sup>FL/+</sup>) with the *Kras*<sup>LSL.G12D/wt</sup> knock-in line (26, 27). The *Kras*<sup>LSL.G12D</sup> knock-in permits tissue-specific expression of a *Kras* allele carrying the highly oncogenic G12D mutation. To induce lung tumors in these mice, we intranasally instilled animals with adenovirus-like particles encoding the Cre recombinase under control of the CMV promoter (AdCre). In this system, mice with a tissue-specific knock-out of all four *Nkiras* alleles (genotype *Nkiras1*<sup>-/-</sup> *Nkiras2*<sup>FL/+</sup> *Kras*<sup>LSL.G12D/wt</sup>; median survival 129 d) succumbed to the lung tumors induced by the AdCre instillation significantly faster than mice retaining a single *Nkiras* allele (*Nkiras1*<sup>-/-</sup> *Nkiras2*<sup>FL/+</sup> *Kras*<sup>LSL.G12D/wt</sup>; median survival 167 d) (Fig. 1A). This was paralleled by markedly earlier onset of weight loss (Fig. 1B and *SI Appendix, Fig. S1A*). Strikingly, the effect of *Nkiras* loss on survival was as profound as the effect of deletion of *Trp53*, which encodes the potent tumor suppressor p53 (genotype *Trp53*<sup>FL/FL</sup> *Kras*<sup>LSL.G12D/wt</sup>; median survival 141 d) (Fig. 1A). These data demonstrate that loss of the  $\kappa$ B-Ras proteins drastically enhances Ras-driven oncogenicity in vivo,

thereby corroborating the results from a recently published mouse model of PDAC (13).

For the AOM/DSS model of colorectal adenocarcinoma (COAD), we combined our cDKO mice with the transgenic villin-Cre line, which expresses Cre under control of the *Vil1* promoter. As loss of  $\kappa$ B-Ras expression is restricted to epithelial cells in these mice (genotype *Nkiras1*<sup>-/-</sup> *Nkiras2*<sup>FL/FL</sup> *Vil1Cre*<sup>tg/0</sup>), our model predicts that tumors will grow faster than in control mice (genotype *Nkiras1*<sup>-/-</sup> *Nkiras2*<sup>FL/FL</sup> or *Nkiras1*<sup>-/-</sup> *Nkiras2*<sup>FL/+</sup> *Vil1Cre*<sup>tg/0</sup>), but exhibit no changes in the extent of inflammation, which is primarily mediated by immune cells, or in the number of tumors. Indeed, we found that the median size of the tumors was significantly increased in cDKO Vil-Cre<sup>+</sup> mice compared to controls (Fig. 1C). This effect became even more apparent when tumors were grouped into diameter bins: The control group had developed substantially more tumors of less than 1 mm in diameter, whereas the cDKO Vil-Cre<sup>+</sup> mice developed correspondingly more tumors larger than 2 mm (Fig. 1D and E). Weight loss, an indicator of the intestinal inflammation driven by DSS administration in this model, was not significantly different between the knock-out mice and controls (*SI Appendix, Fig. S1B*). Similarly, there was no meaningful difference in the total number of tumors between the groups (*SI Appendix, Fig. S1C and D*). Mice exposed to DSS without prior injection of the procarcinogen AOM did not develop tumors but exhibited weight loss indistinguishable from the other two groups, as expected (Fig. 1C and *SI Appendix, Fig. S1B–D*). These results provided in vivo evidence that loss of  $\kappa$ B-Ras expression can have tumor-promoting effects even in the absence of oncogenic *RAS* mutations.

### Loss of the *Nkiras* Genes Promotes a Protumorigenic Transcriptome.

To obtain a better understanding of the global changes that result from loss of the  $\kappa$ B-Ras proteins, we conducted a microarray analysis to determine the transcriptomic differences between mouse embryonic fibroblasts (MEFs) missing all four *Nkiras* alleles (genotype *Nkiras1*<sup>-/-</sup> *Nkiras2*<sup>-/-</sup>; double knock-out, DKO) and MEFs missing only the *Nkiras1* alleles (genotype *Nkiras1*<sup>-/-</sup> *Nkiras2*<sup>+/+</sup>;  $\kappa$ B-Ras 1 single knock-out, 1SKO). These genotypes were chosen as our previous study had shown that  $\kappa$ B-Ras 1 and 2 are functionally redundant, at least in the context of murine Ral activation. Cells were either left untreated or stimulated for 5 h with 100 ng/mL epidermal growth factor (EGF), a potent activator of Ras signaling (*Dataset S1*). To minimize the effects of experimental noise, only genes with a mean expression value exceeding 100 were considered in our subsequent analyses (*SI Appendix, Fig. S2A–D*). Genes that exhibited at least a threefold difference were considered differentially expressed genes (DEGs) (*Datasets S2–S4*). In unstimulated MEFs, we detected 154 DEGs that were down-regulated in DKO cells compared to 1SKO cells, whereas 162 were up-regulated. Under EGF stimulation, far fewer genes were differentially expressed, with 42 genes down-regulated and 38 genes up-regulated in DKO cells (Fig. 2A–C). This result is consistent with our previously reported observation that Ral signaling is strongly activated in DKO cells even in the absence of EGF stimulation. Interestingly, the overall EGF response was drastically different in DKO and 1SKO cells (*SI Appendix, Fig. S2E and F*). The limited overlap in EGF-responsive genes suggests that the high level of background signaling resulting from the absence of  $\kappa$ B-Ras proteins in DKO cells may indeed cause a broad rewiring of the global transcriptome in these cells.

To understand the functional consequences of these transcriptomic changes, we performed Gene Set Enrichment Analysis with preranking based on the fold change between 1SKO and DKO

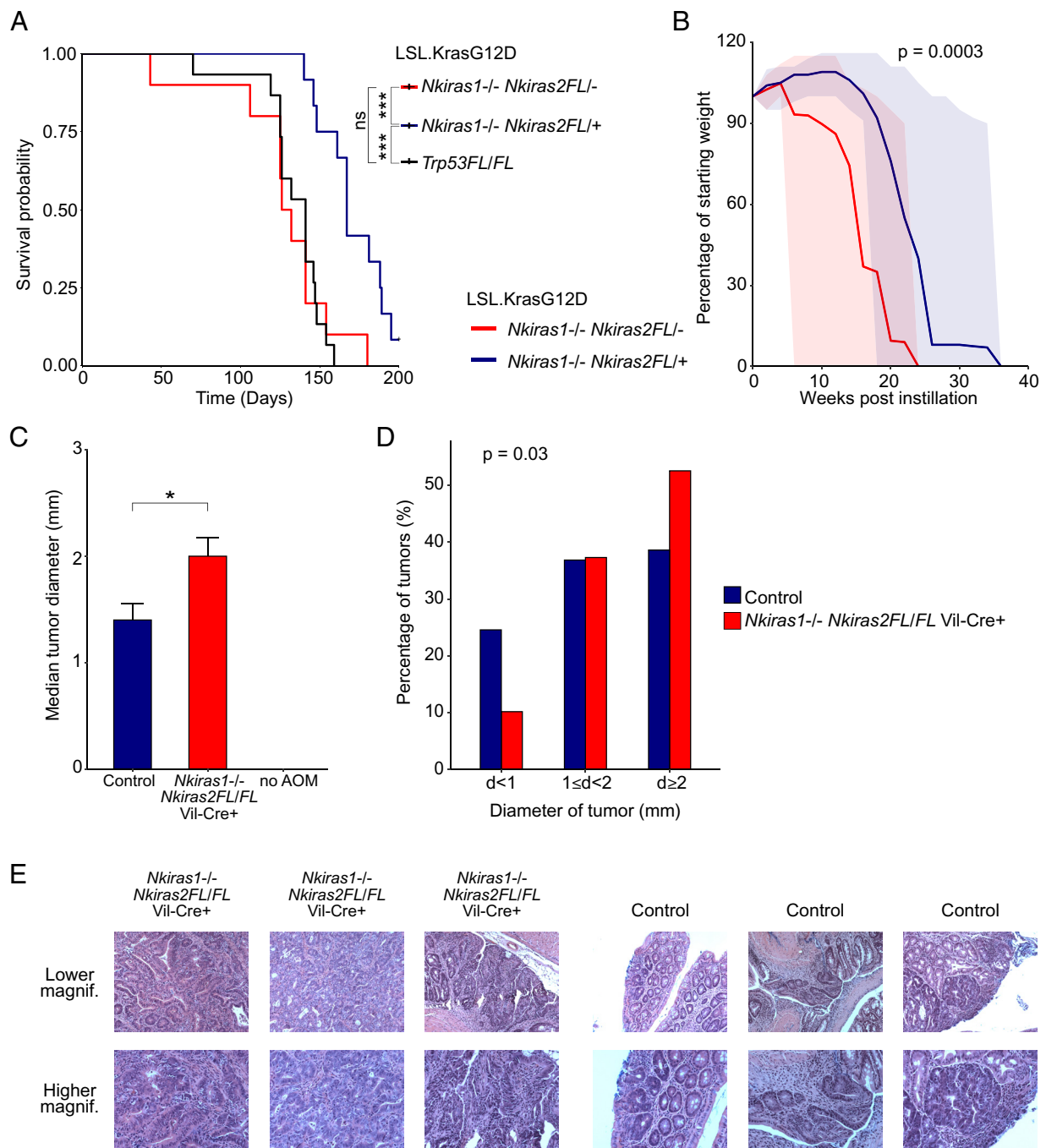


**Fig. 1.** The  $\kappa$ B-Ras proteins exhibit tumor-suppressive properties in two mouse models of cancer. (A and B) Lung tumors induced by intranasal instillation of AdCre in cDKO LSL.K-RasG12D, Ctrl LSL.K-RasG12D, and  $p53^{FL/FL}$  LSL.K-RasG12D mice (10 to 15 mice per group). (A) Survival curve. (B) Weight loss over time.  $P$  value compares the area under the curve for each animal. (C–E) AOM/DSS model of colitis-associated colon cancer in cDKO Vil-Cre<sup>+</sup> and control mice. Colon samples were harvested on day 67 after AOM treatment. Eleven mice per group. (C) Median tumor diameter. (D) Diameter distribution of tumors.  $P$  value reflects comparison of all samples across bins [same as in (C)]. (E) Representative H&E images of colon sections. \*\*\* $P$ -value < 0.001; \* $P$ -value < 0.05; ns, not significant in the Wilcoxon rank-sum test.

cells with and without EGF stimulation. Consistent with our model that  $\kappa$ B-Ras proteins act as dual inhibitors, we found a significant enrichment of genes altered in DKO cells among gene sets related to NF- $\kappa$ B and to Ras signaling, both in the presence and absence of EGF stimulation (Fig. 2 D–G). Furthermore, gene sets related to inflammation and cancer also exhibited significant enrichment (SI Appendix, Fig. S2 G–J). There was substantial overlap between the gene sets showing enrichment with and without EGF treatment, suggesting that loss of  $\kappa$ B-Ras affects similar pathways under both conditions, even in the absence of a major overlap in individual DEGs (SI Appendix, Fig. S2K).

**Expression of *NKIRAS1*, but Not of *NKIRAS2*, Is Frequently and Selectively Down-Regulated in a Broad Range of Human Cancers.** It has been reported previously that *NKIRAS1* expression is reduced in several human cancers, but the relevance of this observation for patient survival has not been explored (12–22). We therefore set out to perform an in-depth, pan-cancer analysis of *NKIRAS1* and *NKIRAS2* using data from more than 10,000 tumor samples representing 32 different human cancers available through The Cancer Genome Atlas (TCGA; Dataset S5). We began by querying the frequency of deletion for *NKIRAS1* and *NKIRAS2*. While homozygous loss of either gene was quite rare



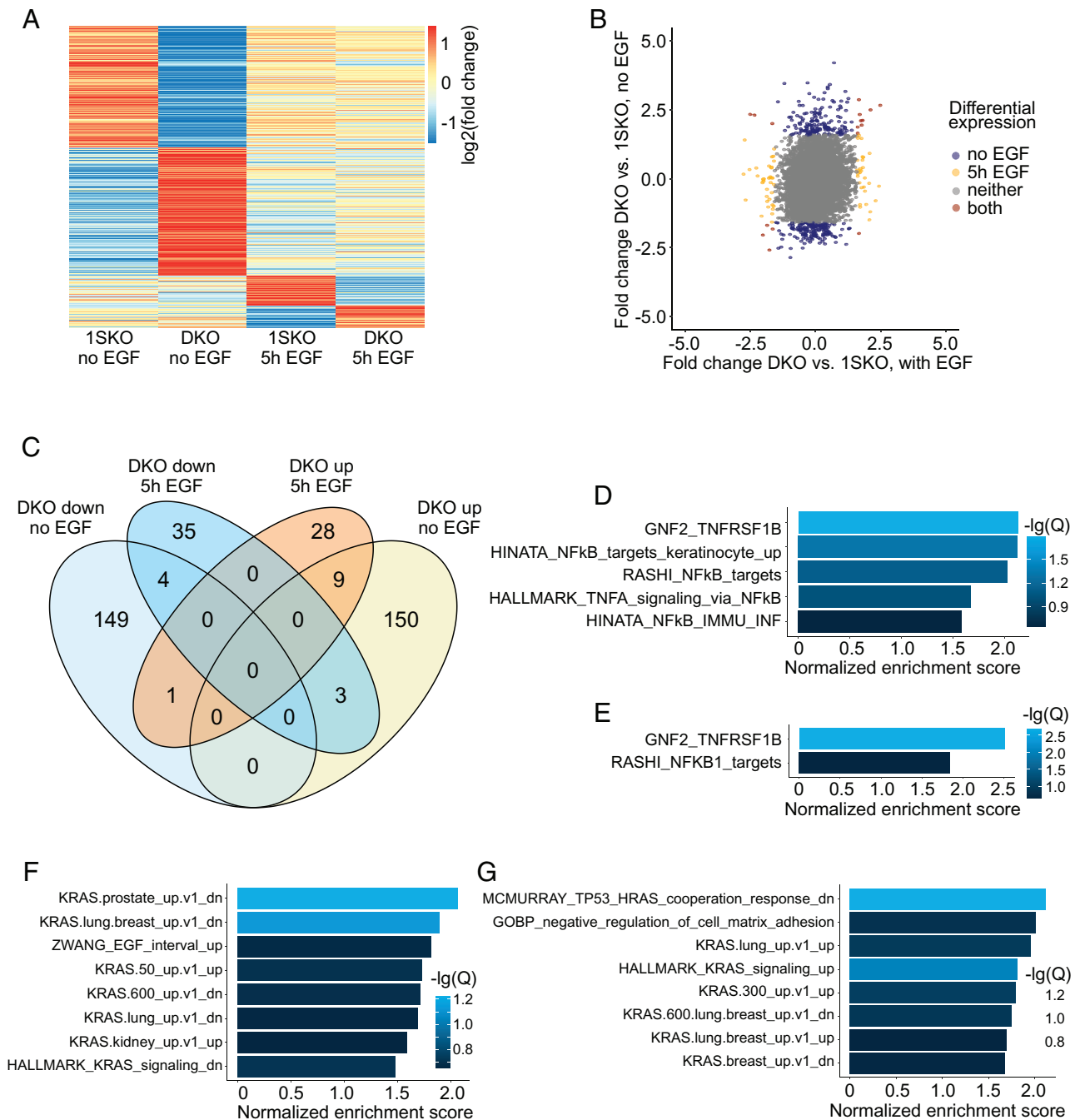


**Fig. 2.** *Nkiras*-deficient MEFs have a generally protumorigenic transcriptome. Microarray of 1SKO and DKO MEFs with and without EGF stimulation. (A) Expression heatmap of DEGs. K-means clustering,  $k = 4$ . (B) Scatter plot of fold changes in DKO MEFs compared to 1SKO MEFs, EGF stimulation vs. no stimulation. (C) Venn diagram of DEGs. (D–G) GSEA normalized enrichment scores (NES) for selected gene sets associated with (D) NF- $\kappa$ B signaling from unstimulated MEFs, (E) NF- $\kappa$ B signaling from EGF-stimulated MEFs, (F) Ras signaling from unstimulated MEFs, and (G) Ras signaling from EGF-stimulated MEFs.

across all cancers investigated, heterozygous loss occurred with exceptionally high frequency. Indeed, six different cancer types exhibited heterozygous loss of *NKIRAS1* in more than 50% of all samples in TCGA, with kidney renal clear cell carcinoma (KIRC) and lung squamous cell carcinoma (LUSC) exhibiting loss in more than 80% of samples (Fig. 3A). Loss of *NKIRAS2* was less prevalent but still rather frequent, with heterozygous loss occurring in more than 70% of samples from patients with ovarian serous cystadenocarcinoma (OV) and kidney chromophobe (KICH) (Fig. 3A). Genomic deletion of either *NKIRAS1* or *NKIRAS2* was associated with worse survival outcomes in an analysis of all available samples regardless of cancer type (Fig. 3B). Surprisingly, however, simultaneous loss of *NKIRAS1* and *NKIRAS2* was

not associated with an additional decrease in patient survival probability, contrary to expectations based on our observations in murine models (Fig. 3B). Occurrence of genomic loss of *NKIRAS1* and *NKIRAS2* was positively associated with high significance but a low odds ratio of only 1.7, suggesting that simultaneous loss of both genes was not common across human cancers (Fig. 3C). Loss of *NKIRAS1* was moderately less likely to occur when tumor samples had mutations in any of the three *RAS* genes and vice versa (Fig. 3C and *SI Appendix, Fig. S3 A–C*). *NKIRAS2* exhibited a similar pattern for *HRAS* and *KRAS*, but no statistical relationship with *NRAS* mutation (Fig. 3D). We also noted a highly significant co-occurrence of deletion or mutation of *TP53*, the gene encoding p53 in humans, and genomic loss of *NKIRAS1* and *NKIRAS2*,

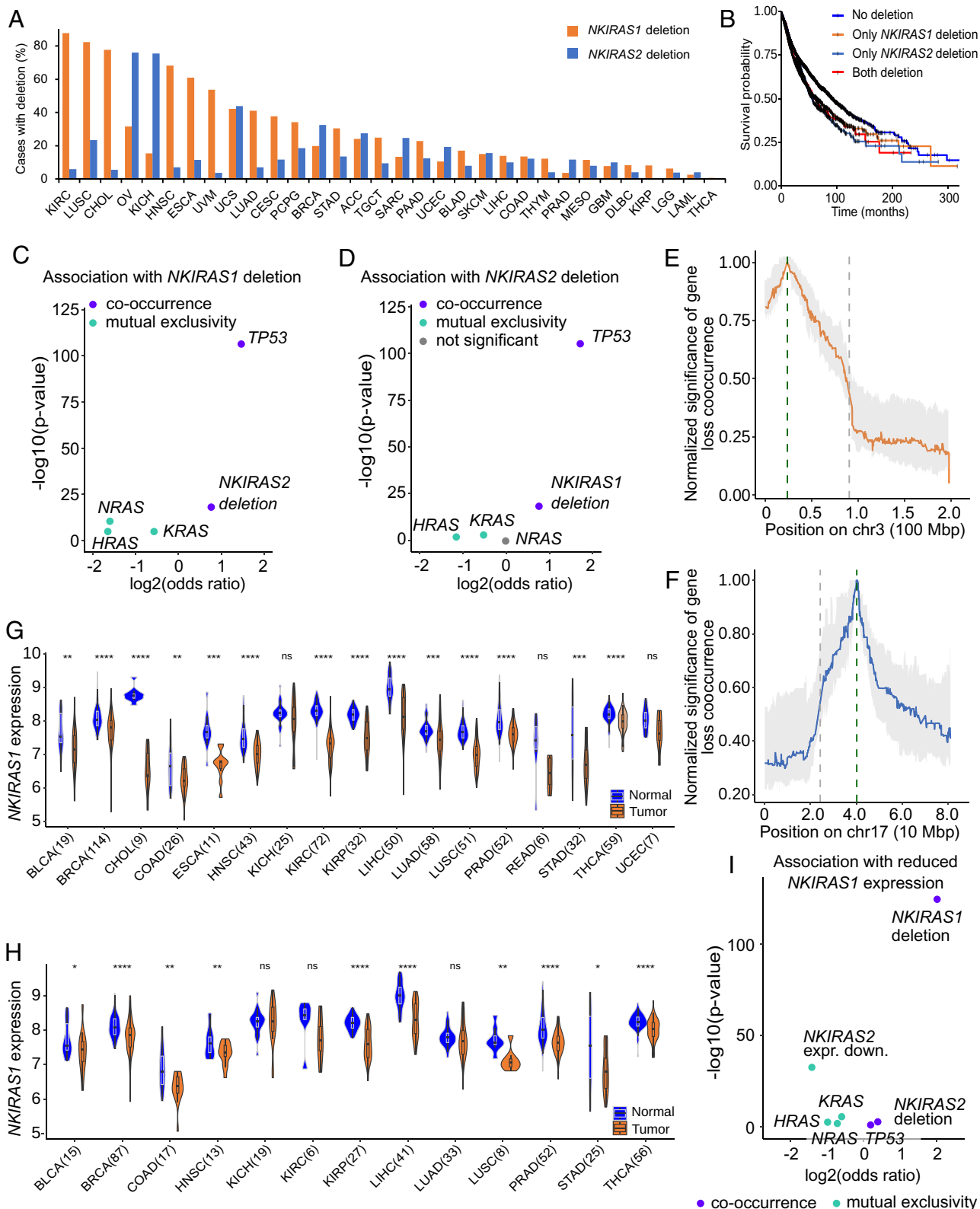


**Fig. 3.** *NKIRAS1*, but not *NKIRAS2*, is commonly down-regulated in human cancers. (A) Prevalence of heterozygous or homozygous genomic deletion of *NKIRAS1* and *NKIRAS2*. (B) Overall survival probability of patients in TCGA, grouped by the presence or absence of genomic deletion of *NKIRAS1* and/or *NKIRAS2*. (C and D) Bubble plots showing likelihood for co-occurrence of genomic loss of (C) *NKIRAS1* and (D) *NKIRAS2* with genomic loss of the other *NKIRAS* gene, mutation of the three *RAS* genes, and mutation or homozygous loss of *TP53*. (E and F) Normalized q-values for the co-occurrence of gene loss of (E) *NKIRAS1* and all other genes on chromosome 3 and of (F) *NKIRAS2* and all other genes on chromosome 17, by location on the respective chromosome. The green dashed line indicates the location of the *NKIRAS* gene; the gray dashed line indicates the location of the centromere. (G and H) Comparison of gene expression levels in tumor tissue and corresponding healthy tissue for *NKIRAS1* (G) in all samples and (H) samples without genomic loss of *NKIRAS1*. (I) Bubble plot showing likelihood for co-occurrence of downregulation of *NKIRAS1* and downregulation of *NKIRAS2*, genomic loss of *NKIRAS1* or *NKIRAS2*, mutation of the three *RAS* genes, and mutation or homozygous loss of *TP53*.

although with a moderately high odds ratio (Fig. 3 C and D and *SI Appendix*, Fig. S3D).

A closer examination of the deletion events in these datasets revealed, however, that in the vast majority of samples, genomic loss of *NKIRAS1* was not focal, but rather associated with loss of a large section of chromosome 3, with breakpoints typically occurring near the centromere (Fig. 3E). Loss of *NKIRAS2* was generally associated with smaller deletions but still difficult to separate from loss of nearby genes on the comparatively small chromosome 17 (Fig. 3F). This lack of regional selectivity prevented us from employing algorithms designed to elucidate the contribution of deletions or mutations in individual genes, such as GISTIC and MutComFocal. We therefore decided to instead utilize expression data for our subsequent analyses, which permits a more localized evaluation.

TCGA contains transcriptomic data from tumor and normal tissue for 17 of the 33 cancer types in its repository (*Dataset S5*). A subset of the data in these 17 studies is derived from paired samples, i.e., biopsies taken from tumor tissue and adjacent healthy tissue of the same patient. We first used these paired samples to determine whether *NKIRAS1* was significantly down-regulated in any tumor tissues. Remarkably, we found that *NKIRAS1* expression was significantly reduced in 14 of the 17 cancer types for which data were available (Fig. 3G). This was also the case for the vast majority of cancer types when only samples without genomic loss of *NKIRAS1* were considered, demonstrating that the down-regulation was not merely the result of a broad and unspecific genomic deletion event. Two of the three tumor types in which *NKIRAS1* was not down-regulated in this analysis, KIRC and lung adenocarcinoma (LUAD), showed a nonsignificant trend toward downregulation (Fig. 3H). Importantly, the genes immediately adjacent to *NKIRAS1* on chromosome 3, *RPL15* and *UBE2E1*, exhibited a starkly different pattern of expression changes in most cancer types, confirming that the changes we observed for *NKIRAS1* were gene-specific and not the result of regional, genomic changes (*SI Appendix*, Fig. S3 E and F). *NKIRAS2* was either unchanged or up-regulated in almost all cancer types with available data, regardless of whether there was genomic loss or not (*SI Appendix*, Fig. S3 G and H). Taken together, these data show that expression of *NKIRAS1*, but not of its flanking genes or of *NKIRAS2*, is reduced selectively in a broad spectrum of tumors. We therefore focused primarily on the role of *NKIRAS1* for the remainder of this study.

Next, we determined whether changes in *NKIRAS1* expression were consistently associated with other transcriptomic or genomic changes. Surprisingly, downregulation of *NKIRAS1* by more than one SD compared to normal tissue (including paired and unpaired samples) was negatively associated with downregulation of *NKIRAS2*, suggesting that simultaneous reduction of the expression of both genes does not provide a significant advantage to tumorigenesis or carcinogenesis (Fig. 3I). Breaking down this analysis by individual cancer types, we found that simultaneous downregulation of *NKIRAS1* and *NKIRAS2* was particularly rare in KIRC and uterine corpus endometrial carcinoma (UCEC). Negative associations were also significant in thyroid carcinoma (THCA), LUAD, and breast invasive carcinoma (BRCA), albeit with more modest odds ratios (*SI Appendix*, Fig. S3I). As observed with genomic deletion, downregulation of *NKIRAS1* was negatively associated with mutation of the three *RAS* genes with modest odds ratios (Fig. 3J). When split up into individual cancer types, significant associations were limited to only very few cancers (*SI Appendix*, Fig. S3 J–L). The positive association with mutation or deletion of *TP53* observed with genomic loss was also detected with *NKIRAS1* downregulation, but with low significance and negligible odds ratios (Fig. 3I and *SI Appendix*, Fig. S3M).

### Downregulation of *NKIRAS1* Is Associated with a Protumorigenic

**Transcriptional Program.** To establish the transcriptional program associated with downregulation of *NKIRAS1* in human tumors, we next determined which genes exhibited an expression pattern correlated positively or negatively with *NKIRAS1* expression across all TCGA cancer types with expression data from normal tissue available. We noticed a substantial enrichment of genes located on chromosome 3 in most tumor types, likely reflecting the frequent, large-scale genomic loss discussed above (Fig. 4A). To minimize this confounding effect, we divided the samples into those with and without genomic loss of *NKIRAS1*, which essentially eliminated the enrichment of genes located on the same chromosome (Fig. 4 B and C and *SI Appendix*, Fig. S4). We then performed an unbiased GSEA analysis using the  $-\log_{10}$ -transformed q-values of the Spearman correlation between *NKIRAS1* expression and all other expressed genes as ranking criterion. As this approach did not require information about *NKIRAS1* expression levels in normal tissue, we were able to include transcriptomic data from all 32 cancer types represented in TCGA. When only samples without genomic loss of *NKIRAS1* were considered, unsupervised clustering by GSEA Hallmark gene sets and by cancer type revealed two distinct clusters: in bladder urothelial carcinoma (BLCA), head and neck squamous cell carcinoma (HNSC), KIRC, LUSC, and OV, *NKIRAS1*-associated genes were enriched in gene sets implicated in epithelial-mesenchymal transition; increased KRAS signaling; and the inflammatory response. Most cancer types in this cluster were additionally associated with target genes of the transcription factor Myc; metabolic signaling, including oxidative phosphorylation, MTORC1 signaling, and adipogenesis; TNF signaling via NF- $\kappa$ B; the IFN- $\gamma$  response; as well as STAT3 and STAT5 signaling. These results are fully consistent with our model of *NKIRAS1* as a tumor-suppressor gene acting by inhibiting both proinflammatory and proliferative signaling. A second cluster including adrenocortical carcinoma, glioblastoma multiforme, KICH, kidney renal papillary cell carcinoma (KIRP), skin cutaneous melanoma (SKCM), UCEC, and uveal melanoma were enriched for genes associated with metabolic signaling, specifically oxidative phosphorylation and the PI3K-AKT-MTOR signaling pathway and DNA repair. Interestingly, BRCA and LUAD formed a miniature cluster with a phenotype in between the first and second cluster. COAD was associated with epithelial-mesenchymal transition, as well as KRAS signaling and Tnf signaling via NF- $\kappa$ B, consistent with the known importance of Ras and NF- $\kappa$ B signaling for this cancer type in humans. Seven cancer types were associated with the G2-M DNA damage checkpoint and the E2F transcription factor (Fig. 4D). When only samples with heterozygous loss of *NKIRAS1* were used in the analysis, two different clusters emerged: BRCA, HNSC, LUAD, KIRC, and SKCM all exhibited highly significant enrichment for genes associated with the G2-M DNA damage checkpoint; the E2F transcription factor family; and regulation of the mitotic spindle apparatus. The same cluster also exhibited less tight associations with DNA repair; PI3K-AKT-MTOR signaling; and targets of the oncogenic transcription factor Myc. A second, looser cluster consisted of cholangiocarcinoma (CHOL), liver hepatocellular carcinoma (LIHC), lower grade glioma (LGG), LUSC, pheochromocytoma and paraganglioma (PCPG), and testicular germ cell tumors (TGCT), and was associated with epithelial-mesenchymal transition; glycolysis; and hypoxia. LIHC, LGG, and PCPG were also associated with increased KRAS signaling. COAD exhibited particularly significant enrichment for genes involved in epithelial-mesenchymal transition (Fig. 4E). Of note, a total of 15 individual cancer types were

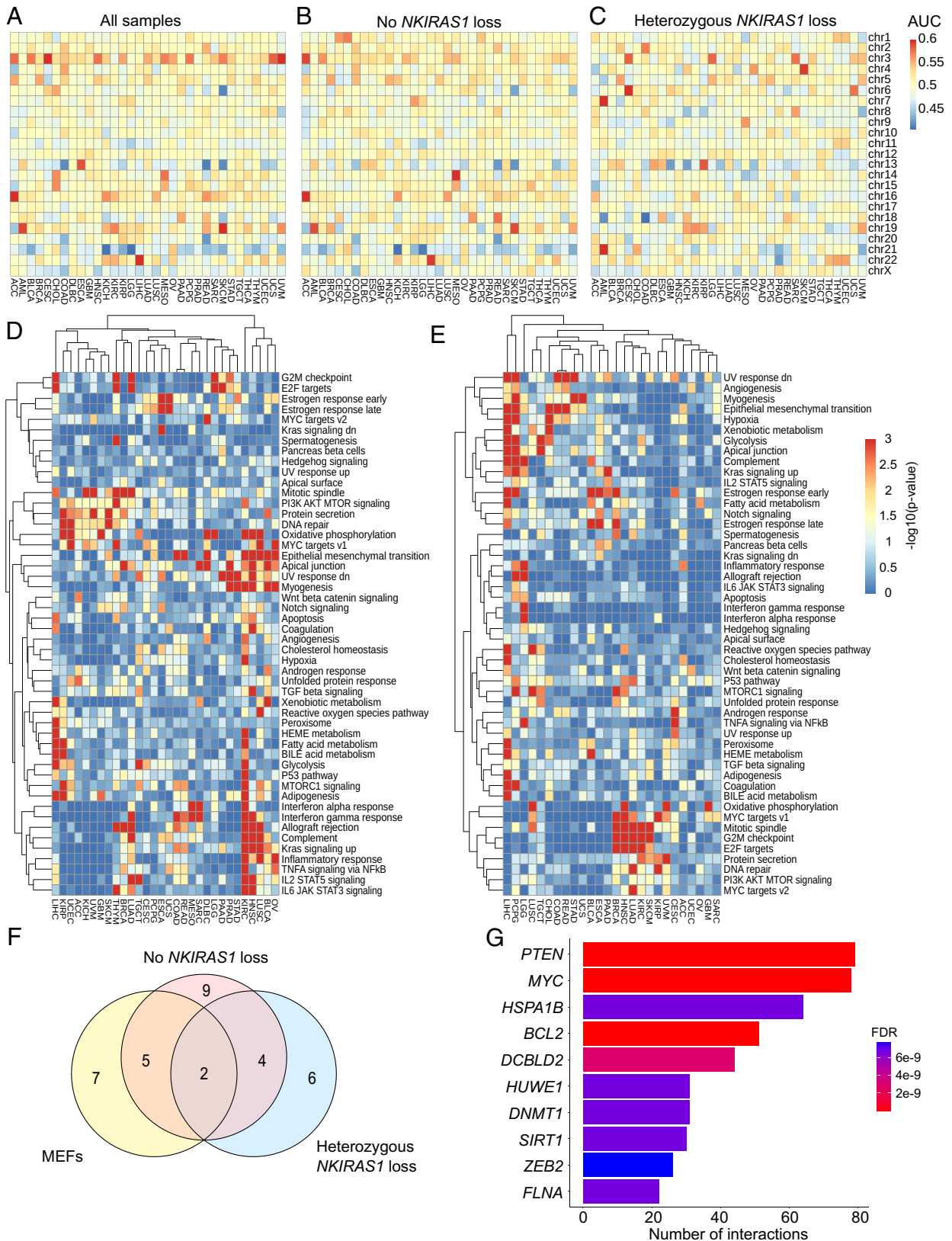


**Fig. 4.** The transcriptional program in cancers with reduced *NKIRAS1* expression is generally more protumorigenic. (A–C) Heatmaps showing the area under the curve (AUC) of all human genes ranked by the q-value of their coexpression with *NKIRAS1* and their chromosomal location for (A) all samples, (B) only samples without genomic loss of *NKIRAS1*, and (C) only samples with heterozygous loss of *NKIRAS1*. (D and E) Heatmaps of the negative log-transformed *P*-value for enrichment in the GSEA Hallmark gene sets for genes ranked by the negative log-transformed q-value of their correlation with *NKIRAS1* across TCGA tumors for samples (D) without genomic loss of *NKIRAS1* and (E) with heterozygous loss of *NKIRAS1*. (F) Venn diagram showing the number of GSEA categories that overlapped between the DKO MEF microarray results and the two clusters each in TCGA samples with and without heterozygous loss of *NKIRAS1*. (G) Ten genes most commonly targeted by miRNAs whose expression correlated with *NKIRAS1* in at least one TCGA cancer type. Color corresponds to FDR for association between *NKIRAS1* and the respective gene.



enriched for genes associated with epithelial-mesenchymal transition among samples with heterozygous *NKIRAS1* loss, without loss, or among both of these groups with a *P*-value < 0.01. This is consistent with the importance of Ral signaling in this particular biological process. The most notable difference between the association clusters of samples without genomic loss of *NKIRAS1* and those with heterozygous loss was that gene sets related to inflammatory signaling or NF- $\kappa$ B signaling were completely missing from the latter. This discrepancy likely reflects the effects of loss of large sections of chromosome 3 along with the *NKIRAS1* gene locus, which are liable to alter the overall signaling landscape of the tumor cell (Fig. 3E). Strikingly, there was extensive overlap between the Hallmark GSEA sets altered in DKO MEFs and those in the two clusters of tumors without genomic loss of *NKIRAS1*, consistent with a model in which loss of *NKIRAS1* expression is indeed a driving force behind at least some of these changes, not just a side effect (Figs. 2 D–G and 4F and SI Appendix, Fig. S2 G–J). An analogous analysis of microRNAs (miRNAs) identified 693 miRNAs whose expression significantly correlated, positively or negatively, with *NKIRAS1* in at least one cancer type (q-value < 10<sup>-4</sup>). Intriguingly, the ten genes targeted most frequently by these miRNAs included several key regulators of proliferation, transcription, survival, and carcinogenesis, most notably *PTEN*, *MYC*, and *BCL2*, as well as the gene encoding the NF- $\kappa$ B inhibitor sirtuin 1 (Fig. 4G).

Taken together, these findings are consistent with a generally protumorigenic transcriptional profile associated with the downregulation of *NKIRAS1* expression across a multitude of human tumors

**Changes in *NKIRAS1* Levels in Tumors Are Not Associated with Changes in DNA Methylation.** The expression of tumor-suppressor genes is often selectively reduced in human cancers by one or more of three distinct mechanisms: genomic deletion; promoter methylation; or upregulation of miRNAs targeting the tumor-suppressor gene. As our analysis had revealed that *NKIRAS1* expression was reduced across many cancers independently of genomic deletion (Fig. 3H), we first investigated the possibility of DNA methylation. The TCGA DNA methylation dataset contains 16 experimentally validated methylation sites that fall within a region encompassing the gene body of *NKIRAS1* and 800 bp upstream of its transcriptional start site. The first 14 of these sites, cg18328135 through cg12117273, form a tight cluster that falls within the promoter region and the first exon of *NKIRAS1*. All of these sites are consistently hypomethylated, with a beta value below 0.1. The two remaining sites, which are located deep within intron 1 (cg11233163) and toward the end of the *NKIRAS1* gene (cg23019576), are generally hypermethylated with beta values typically well above 0.5 regardless of tumor type, with some exceptions in which cg11233163 exhibits values closer to 0.25. When we directly compared the methylation values in samples from tumors with reduced expression of *NKIRAS1* (relative to healthy tissue) with samples from tumors without downregulation of *NKIRAS1*, we found several instances in which individual methylation sites exhibited different beta values between both groups, often with increased methylation in the samples with reduced *NKIRAS1* levels. However, these differences, while statistically significant, were comparatively minor and unlikely to meaningfully alter *NKIRAS1* expression. The exception from this was cg11233163, which showed considerable methylation increases in KICH, KIRC, KIRP, LIHC, and UCEC. However, its location well inside the gene body made it unlikely to serve as a major regulator of *NKIRAS1* expression (SI Appendix, Fig. S5).

We therefore effectively excluded DNA methylation as a possible explanation for the reduced expression of *NKIRAS1*.

**Changes in *NKIRAS1* Levels in Tumors Are Associated with a miRNA Regulatory Network.** Next, we examined the role of miRNAs in the expression of *NKIRAS1*. A search of miRTarBase, a comprehensive miRNA database, revealed that of the 693 miRNAs exhibiting expression patterns correlated with *NKIRAS1* levels, 11 were predicted to directly target the 3'-UTR of *NKIRAS1* at two different locations (Fig. 5A). Four of these miRNAs (miR-17-5p, miR-20a-5p, miR-93-5p, and miR-106b-5p) formed a remarkably tight cluster that was negatively correlated with *NKIRAS1* in up to 22 different tumor types. A second cluster, consisting of miR-526b-3p and four members of the miR-519 family, showed a particularly consistent negative correlation with *NKIRAS1* in TGCT. The two remaining miRNAs, miR-20b-5p and miR-106a-5p, formed an intermediate between these two larger clusters (Fig. 5B). This consistent occurrence of a negative correlation across multiple tumors suggests that tumors may indeed up-regulate miRNAs to decrease *NKIRAS1* expression. As miRNAs typically function by targeting gene networks, rather than individual genes, we next determined whether the miRNAs targeting *NKIRAS1* were predicted to also target additional genes. Indeed, we found that all of these 11 miRNAs targeted the same set of 23 genes in addition to *NKIRAS1*. These additional targets included several genes whose products have been implicated in tumorigenesis, including *ARID4B*, *USP32*, *EMSY*, *HMGB3*, *TSG101*; mTOR-associated genes *LAMTOR1* and *STK11IP*; and *TAX1BP1*, which encodes a protein inhibitor of NF- $\kappa$ B activation (Fig. 5C). If *NKIRAS1* is in fact part of a larger gene network regulated by this set of 11 miRNAs, there should be a positive correlation between the expression levels of *NKIRAS1* and the other target genes in at least a subset of tumors. We therefore determined the correlation between *NKIRAS1* and each of the 23 additional genes in the network and found that all of them exhibited expression positively correlated with *NKIRAS1* levels in at least two (*STK11IP*) and up to 27 (*C3ORF38*, *TAX1BP1*, and *TMEM242*) different tumor types in samples with and without genomic loss of *NKIRAS1* (SI Appendix, Fig. S6). To understand whether these correlation patterns were statistically significant and likely to reflect a meaningful biological mechanism, we performed 1,000 iterations of randomly sampling 23 genes and calculating the sum of the Spearman coefficients for the correlation between their expression and *NKIRAS1* expression, thus establishing a random-case distribution separately for each tumor type and for samples with and without genomic loss of *NKIRAS1*. The sum of correlation coefficients for the 23 genes targeted by miRNAs that were both *NKIRAS1*-associated and *NKIRAS1*-targeting had a positive z-score in the vast majority of tumors, suggesting that *NKIRAS1* is indeed targeted as part of this larger gene network (Fig. 5D).

While not predicted to be a direct target, *NKIRAS1* expression has been shown previously to be reduced by miR-155, a mechanism that promotes NF- $\kappa$ B activation during hematopoiesis (28). We therefore assessed the correlation of miR-155 and *NKIRAS1* and found that it was indeed significant in a number of human tumors, for both miR-155-5p and miR-155-3p (Fig. 5E and F). Therefore, miR-155 may act as another, likely indirect miRNA regulator of *NKIRAS1* in a subset of human cancers.

These results suggest that the widespread downregulation of *NKIRAS1* across human tumors is mediated, at least in part, by a network of miRNAs, and that *NKIRAS1* itself is part of a larger network of target genes regulated in a coordinated fashion.



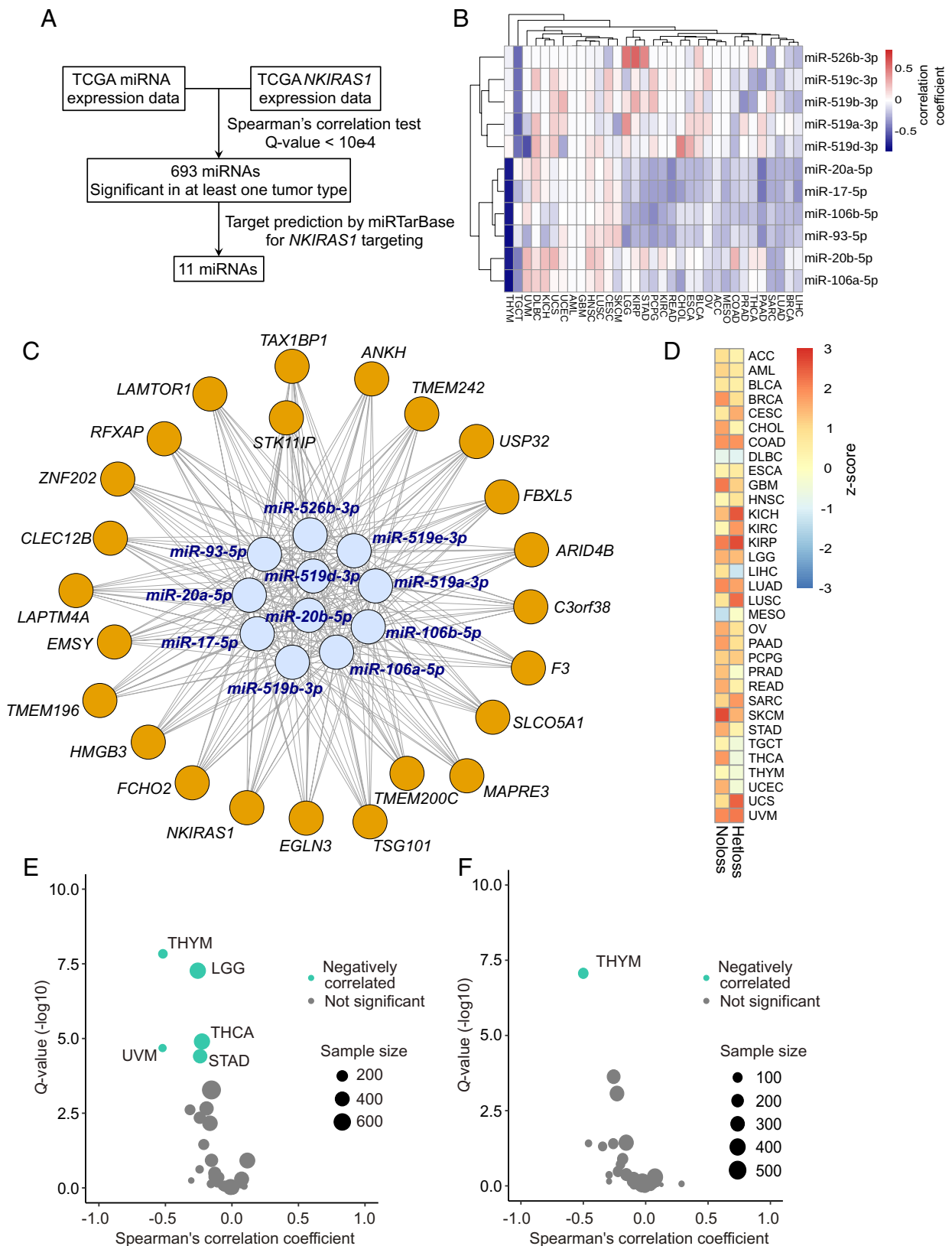


**Fig. 5.** *NKIRAS1* expression is associated with a miRNA regulatory network in human tumors. (A) Flow chart summarizing the filtering approach to identify relevant *NKIRAS1*-targeting miRNAs. (B) Spearman correlation between the 11 *NKIRAS1*-targeting and *NKIRAS1*-associated miRNAs in each cancer type. (C) Interactome representing the network of 24 genes targeted by the 11 *NKIRAS1*-targeting and *NKIRAS1*-associated miRNAs. (D) Heatmap showing the Z-scores of the sum of Spearman coefficients for the correlation between the expression of *NKIRAS1* and the other 23 genes targeted by the same miRNAs relative to the median of 1,000 sets of 23 randomly sampled genes. (E and F) Bubble plots showing the sample size, Spearman correlation coefficient and the associated q-value of *NKIRAS1* and (E) miR-155-5p and (F) miR-155-3p. Tumor types with significant correlation are shown in turquoise.

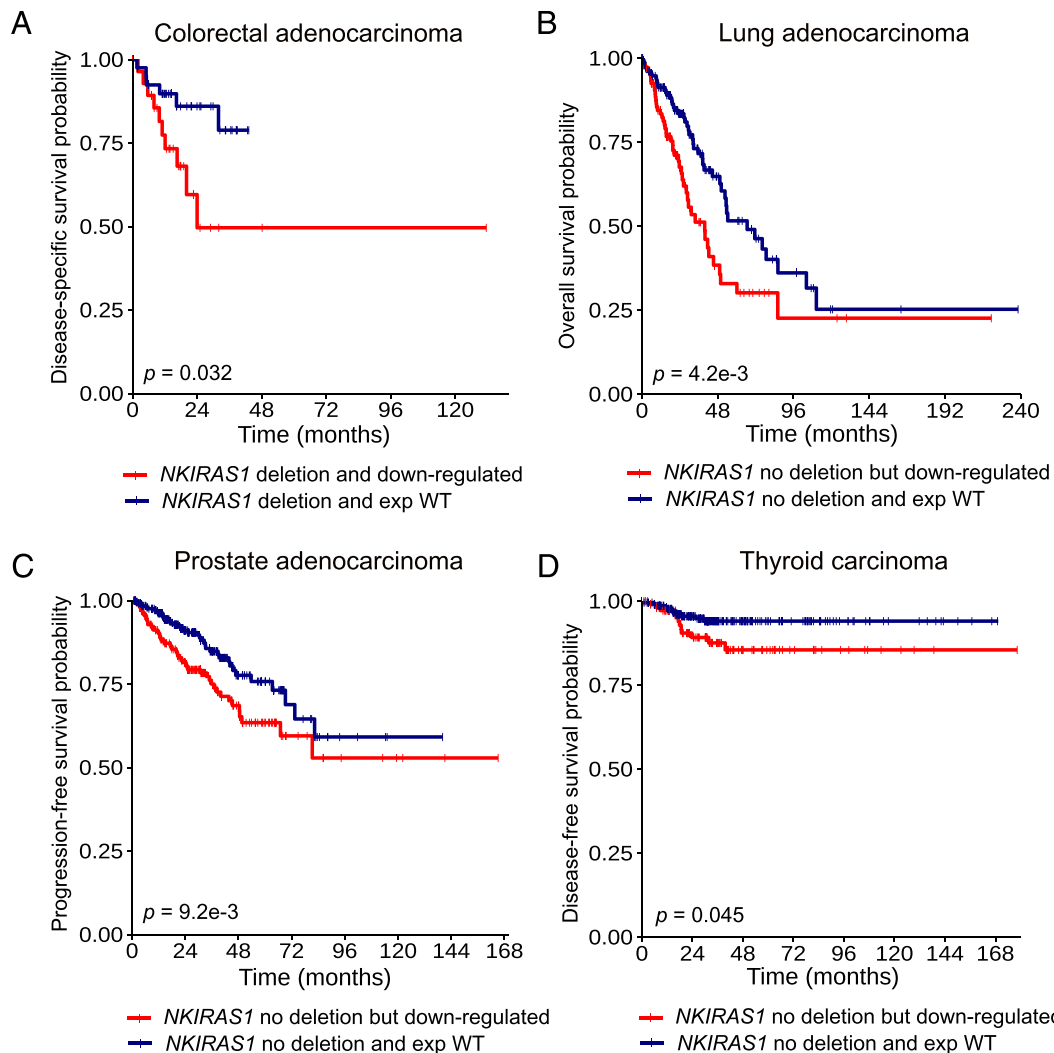


**Fig. 6.** Downregulation of *NKIRAS1*, but not *NKIRAS2*, is associated with poor prognosis in several human cancers. Survival of patients with or without downregulation of *NKIRAS1* in (A) COAD (disease-specific survival), (B) LUAD (overall survival), (C) PRAD (progression-free survival), and (D) THCA (disease-free survival).

**Downregulation of *NKIRAS1*, but Not *NKIRAS2*, Is Associated with Poor Prognosis in Several Human Cancers.** To understand whether the frequent and selective reduction of *NKIRAS1* expression across cancer types, and the associated transcriptomic changes, have clinical relevance, we asked whether *NKIRAS1* downregulation was correlated with patient survival. Samples were binned into those with and without loss of the *NKIRAS1* gene locus and the bins processed independently. Reduced *NKIRAS1* expression was significantly associated with shorter survival in four human cancers: COAD, LUAD, prostate adenocarcinoma (PRAD), and THCA (Fig. 6). In contrast, downregulation of *NKIRAS2*, *RPL15*, or *UBE2E1* was not associated with shorter survival in the available datasets (SI Appendix, Fig. S7). An analogous analysis of the genes targeted along with *NKIRAS1* by the same miRNA network indicated that several of them were associated with shortened survival in the same tumor types (SI Appendix, Fig. S8). However, this was not observed consistently across all genes and tumor types, suggesting that the effect of *NKIRAS1* downregulation was not predicated on downregulation (or expression) of the genes cotargeted by the same miRNA network.

Together, these data reveal an unexpected, widespread and specific downregulation of *NKIRAS1* expression in a broad range of human cancers, which is associated with worse prognosis for several tumor types. Surprisingly, this downregulation occurs only

very rarely in conjunction with mutations of the *RAS* genes or loss of *NKIRAS2* expression, suggesting that the role of *NKIRAS1* as a tumor suppressor is broader in humans than previously assumed based on mouse models.

## Discussion

The  $\kappa$ B-Ras proteins function as inhibitors of NF- $\kappa$ B activation and Ral signaling. This central positioning within two largely independent pathways that are closely associated with carcinogenesis implicates them as potential tumor suppressors. While the molecular mechanisms underlying the inhibitory function of the  $\kappa$ B-Ras proteins have been thoroughly studied, it has remained largely unexplored whether these properties translate to tumor-suppressive capacity with broad physiological relevance for carcinogenesis. Indeed, although reduced expression of *NKIRAS1* and *NKIRAS2* has been noted previously in a variety of tumor types, the consequences of this phenomenon have only been investigated carefully in the context of PDAC, with the use of a K-Ras<sup>G12D</sup>-driven mouse model, murine organoid cultures, and human PDAC biopsies. In that study, we noted an association between reduced  $\kappa$ B-Ras protein levels and advanced disease stage, which was the first time  $\kappa$ B-Ras expression was tied to a clinical outcome (13). Here, we build upon and expand those findings

by examining the role of  $\kappa$ B-Ras expression in a pan-cancer context.

The markedly reduced survival time of cDKO mice we observed in the K-Ras<sup>G12D</sup>-driven model of lung cancer is consistent with the results reported with the PDAC mouse model and further corroborates the role of the  $\kappa$ B-Ras proteins as negative regulators of Ras-driven tumor growth (13). The extent of this effect, which is comparable to that seen upon p53 loss, highlights the potency of  $\kappa$ B-Ras proteins as tumor suppressors. By contrast, our findings with the AOM/DSS model provide *in vivo* evidence that loss of  $\kappa$ B-Ras expression can also promote tumor growth in inflammation-driven, Ras-independent tumors, as this animal model rarely develops spontaneous *Ras* mutations, an important difference to colorectal cancer in humans (23–25). This observation considerably broadens the relevance of  $\kappa$ B-Ras proteins as tumor suppressors beyond only Ras-driven cancers. Tumorigenesis in the AOM/DSS model is entirely dependent on intestinal inflammation induced by DSS, as mice do not develop tumors after injection of AOM alone. The tumor microenvironment in this model includes a high concentration of proinflammatory cytokines, which promote cellular proliferation and survival of intestinal epithelial cells, and thereby incipient tumor cells, through the activation of NF- $\kappa$ B signaling, as demonstrated by Greten et al. (29). It is therefore likely that the increase in median tumor size we have observed results from activation of this pathway. However, we have previously shown that Ral signaling is elevated in  $\kappa$ B-Ras-deficient cells even in the absence of Ras activation by stimulation or mutation, indicating that this pathway might also play a role in such a setting (12). Further experiments will determine whether this increase in tumor growth results from the excessive activation of Ral, NF- $\kappa$ B, a third pathway, or a combination of these possibilities.

We have previously reported a high level of functional redundancy between  $\kappa$ B-Ras 1 and  $\kappa$ B-Ras 2, in particular in the context of Ras signaling (12, 13). The presence of either of these proteins was sufficient to effect a complete rescue of the DKO phenotype in a variety of experimental settings, wherefore we considered 1SKO MEFs equivalent to wild-type cells in the microarray experiment.  $\kappa$ B-Ras 1 and  $\kappa$ B-Ras 2 are highly conserved between humans and mice, with sequence identities of 95% and 99%, respectively. We therefore expected that human tumors would exhibit downregulation of both  $\kappa$ B-Ras isoforms in tandem and for this to be tightly associated with oncogenic *RAS* mutations. The finding that coordinated downregulation of *NKIRAS1* and *NKIRAS2* is in fact extremely rare, and that reduced expression of neither is associated with *RAS* mutations, emphasizes the importance of validating findings from murine models with human data. This task was complicated by the high frequency of large-scale deletions on chromosome 3 in many cancers, preventing a clear separation between loss of *NKIRAS1* and the large number of genes on the same chromosomal arm. However, the use of transcriptomic data subgrouped by the presence or absence of heterozygous deletion enabled us to circumvent this problem and establish that *NKIRAS1*, but not the genes adjacent to it on chromosome 3 or its paralog *NKIRAS2*, were commonly down-regulated in a wide variety of human cancers. The fact that this downregulation was associated with poorer patient outcomes in four distinct human cancer types indicates that *NKIRAS1* is a pathophysiologically important tumor-suppressor gene. This hypothesis is further strengthened by the association of *NKIRAS1* downregulation with tumor-promoting transcriptomic changes. While there was no single gene set altered across all investigated cancer types, the emergence of clusters with similar

changes is notable, as it suggests that *NKIRAS1* downregulation forms part of a larger transcriptional program that facilitates tumor growth. The difference in clusters between samples with and without genomic loss of *NKIRAS1*, and thereby of large sections of chromosome 3, likely reflects the effects of other genes lost along with *NKIRAS1* and provides further support for our approach to perform separate analyses of these sample subsets. It is interesting to note that there was considerable overlap in the gene sets enriched for genes associated with *NKIRAS1* loss in human tumors and DEGs from the comparison of 1SKO and DKO MEFs. This observation is consistent with our updated model, which posits that the two  $\kappa$ B-Ras proteins are functionally fully redundant in mice, but that in humans  $\kappa$ B-Ras 1 (*NKIRAS1*) generally assumes a more dominant tumor-suppressive role than  $\kappa$ B-Ras 2 (*NKIRAS2*).

Our results conclusively demonstrate that *NKIRAS1* is frequently down-regulated even in the absence of genomic deletion. While the exact mechanism remains to be determined, DNA methylation does not appear to be a significant factor. The finding that *NKIRAS1* levels are tightly associated with a network of 11 *NKIRAS1*-targeting miRNAs with tumor-specific expression patterns suggests that tumors may evolve to up-regulate a tissue-specific subset of these miRNAs to reduce levels of  $\kappa$ B-Ras 1, along with a network of other targets, and thus promote tumor growth. Further experiments will be necessary to determine the relative contributions and synergistic effects of these miRNAs in different tumor types.

Taken together, the findings presented in this report further corroborate the role of the  $\kappa$ B-Ras proteins as tumor suppressors and reveal the unique importance of  $\kappa$ B-Ras 1 in human cancers. This elevated pathophysiological importance of  $\kappa$ B-Ras 1 was not predicted by our previous results in murine models of cancer and emphasizes the importance of corroborating findings in mouse models of cancer with evidence from human data.

## Methods Summary

Detailed methods are provided in *SI Appendix*.

**Animals and Mouse Models.** All mice in this study were of the C57BL/6J strain. Mice were housed in specific-pathogen-free animal care facilities at Columbia University Irving Medical Center, accredited by the Association for Assessment and Accreditation of Laboratory Animal Care. All mouse experiments described in this study were approved by the Institutional Animal Care and Use Committee of Columbia University. The constitutive knockout of *Nkiras1* and the conditional knockout of *Nkiras2* have been reported in detail previously (12, 13). The *Trp53<sup>fl</sup>* mice were a generous gift from Wei Gu (Columbia University). The *Kras<sup>LSL.G12D</sup>* mice were obtained from the NCI Mouse Repository (# 01XJ6) (26). Villin-Cre mice were purchased from The Jackson Laboratory (# 021504; Bar Harbor, ME, USA) (30). For the lung cancer model, mice were instilled intranasally with AdCre as described previously (27). For the AOM/DSS model of colon cancer, mice were injected with AOM, followed by three cycles of DSS with drinking water followed by rest. The size and number of tumors were determined in a blinded fashion by a pathologist.

**RNA Isolation and Microarray Analysis.** Generation of the MEFs used in this study has been reported previously (12). Transcriptomic changes following EGF stimulation were assessed with a NimbleGen Mouse 12x135K array. Microarray data have been deposited in the Gene Expression Omnibus database ([GSE216127](https://www.ncbi.nlm.nih.gov/geo/query/acc.cgi?acc=GSE216127)) (31). Gene set enrichment was assessed by GSEA (32, 33).

**TCGA Analysis.** Human data were derived from TCGA PanCancer Atlas Studies. Data were retrieved through cBioPortal and the UCSC Xena Functional



Genomics Explorer (34–36). The MIENTURNET platform was used with the miRtarBase database to identify the predicted target genes of *NKIRAS1*-correlated miRNAs (37). A detailed description of the analysis methodology is provided in *SI Appendix*.

**Data, Materials, and Software Availability.** Raw microarray data have been deposited in GEO ([GSE216127](https://www.ncbi.nlm.nih.gov/geo/query/acc.cgi?acc=GSE216127)) (31).

**ACKNOWLEDGMENTS.** We wish to thank Drs. Richard Carvajal and Grazia Ambrosini for productive discussions, expert advice, and experimental support. This work was supported by Deutsche Forschungsgemeinschaft grant

PO 1946/1-1 to T.S.P., by NIH grant R35CA253126 to R.R., and by NIH grant R01CA206556 to S.G.

Author affiliations: <sup>a</sup>Department of Microbiology and Immunology, Vagelos College of Physicians and Surgeons, Columbia University Irving Medical Center, New York, NY 10032; <sup>b</sup>Program for Mathematical Genomics, Department of Systems Biology, Columbia University, New York, NY 10032; <sup>c</sup>Department of Biomedical Informatics, Columbia University, New York, NY 10032; <sup>d</sup>Division of Digestive and Liver Diseases, Department of Medicine, College of Physicians and Surgeons, Columbia University Irving Medical Center, New York, NY 10032; and <sup>e</sup>Department of Pathology and Cell Biology, Columbia University Irving Medical Center, New York, NY 10032

1. I. A. Prior, F. E. Hood, J. L. Hartley, The frequency of Ras mutations in cancer. *Cancer Res.* **80**, 2969–2974 (2020).
2. S. Mukhopadhyay, M. G. Vander Heiden, F. McCormick, The metabolic landscape of RAS-driven cancers from biology to therapy. *Nat. Cancer* **2**, 271–283 (2021).
3. L. H. Apken, A. Oeckinghaus, The RAL signaling network: Cancer and beyond. *Int. Rev. Cell Mol. Biol.* **361**, 21–105 (2021).
4. A. Oeckinghaus, S. Ghosh, The NF- $\kappa$ B family of transcription factors and its regulation. *Cold Spring Harb. Perspect. Biol.* **1**, a000034 (2009).
5. T. S. Postler, S. Ghosh, Bridging the gap: A regulator of NF- $\kappa$ B linking inflammation and cancer. *J. Oral. Biosci.* **57**, 143–147 (2015).
6. C. Fenwick *et al.*, A subclass of Ras proteins that regulate the degradation of I $\kappa$ B. *Science* **287**, 869–873 (2000).
7. F. Sarais *et al.*, Characterisation of the teleostean  $\kappa$ B-Ras family: The two members NKIRAS1 and NKIRAS2 from rainbow trout influence the activity of NF- $\kappa$ B in opposite ways. *Fish Shellfish Immunol.* **106**, 1004–1013 (2020).
8. Y. Chen, J. Wu, G. Ghosh, KappaB-Ras binds to the unique insert within the ankyrin repeat domain of I $\kappa$ B $\beta$  and regulates cytoplasmic retention of I $\kappa$ B $\beta$  x NF- $\kappa$ B complexes. *J. Biol. Chem.* **278**, 23101–23106 (2003).
9. Y. Chen *et al.*, Inhibition of NF- $\kappa$ B activity by I $\kappa$ B $\beta$  in association with kappaB-Ras. *Mol. Cell Biol.* **24**, 3048–3056 (2004).
10. K. Tago, M. Funakoshi-Tago, M. Sakinawa, N. Mizuno, H. Itoh, KappaB-Ras is a nuclear-cytoplasmic small GTPase that inhibits NF- $\kappa$ B activation through the suppression of transcriptional activation of p65/RelA. *J. Biol. Chem.* **285**, 30622–30633 (2010).
11. T. Huxford, G. Ghosh, Inhibition of transcription factor NF- $\kappa$ B activation by kappaB-Ras. *Methods Enzymol.* **407**, 527–534 (2006).
12. A. Oeckinghaus *et al.*,  $\kappa$ B-Ras proteins regulate both NF- $\kappa$ B-dependent inflammation and Ras-dependent proliferation. *Cell Rep.* **8**, 1793–1807 (2014).
13. S. Beel *et al.*,  $\kappa$ B-Ras and Ral GTPases regulate acinar to ductal metaplasia during pancreatic adenocarcinoma development and pancreatitis. *Nat. Commun.* **11**, 3409 (2020).
14. G. Finak *et al.*, Stromal gene expression predicts clinical outcome in breast cancer. *Nat. Med.* **14**, 518–527 (2008).
15. A. E. Karnoub *et al.*, Mesenchymal stem cells within tumour stroma promote breast cancer metastasis. *Nature* **449**, 557–563 (2007).
16. M. E. Garber *et al.*, Diversity of gene expression in adenocarcinoma of the lung. *Proc. Natl. Acad. Sci. U.S.A.* **98**, 13784–13789 (2001).
17. A. Murat *et al.*, Stem cell-related “self-renewal” signature and high epidermal growth factor receptor expression associated with resistance to concomitant chemoradiotherapy in glioblastoma. *J. Clin. Oncol.* **26**, 3015–3024 (2008).
18. L. Sun *et al.*, Neuronal and glioma-derived stem cell factor induces angiogenesis within the brain. *Cancer Cell* **9**, 287–300 (2006).
19. H. Lin *et al.*, Prognostic significance of kappaB-Ras1 expression in gliomas. *Med. Oncol.* **29**, 1272–1279 (2012).
20. G. V. Gerashchenko *et al.*, Genetic and epigenetic changes of NKIRAS1 gene in human renal cell carcinomas. *Exp. Oncol.* **32**, 71–75 (2010).
21. Y.-J. Jou *et al.*, Proteomic identification of salivary transferrin as a biomarker for early detection of oral cancer. *Anal. Chim. Acta* **681**, 41–48 (2010).
22. S. M. Kim *et al.*, Prognostic biomarkers for esophageal adenocarcinoma identified by analysis of tumor transcriptome. *PLoS One* **5**, e15074 (2010).
23. P. E. Jackson, D. P. Cooper, P. J. O’Connor, A. C. Povey, The relationship between 1,2-dimethylhydrazine dose and the induction of colon tumours: Tumour development in female SWR mice does not require a K-ras mutational event. *Carcinogenesis* **20**, 509–513 (1999).
24. M. Takahashi, K. Wakabayashi, Gene mutations and altered gene expression in azoxymethane-induced colon carcinogenesis in rodents. *Cancer Sci.* **95**, 475–480 (2004).
25. Q. Pan *et al.*, Genomic variants in mouse model induced by azoxymethane and dextran sodium sulfate improperly mimic human colorectal cancer. *Sci. Rep.* **7**, 25 (2017).
26. E. L. Jackson *et al.*, Analysis of lung tumor initiation and progression using conditional expression of oncogenic K-ras. *Genes Dev.* **15**, 3243–3248 (2001).
27. M. DuPage, A. L. Dooley, T. Jacks, Conditional mouse lung cancer models using adenoviral or lentiviral delivery of Cre recombinase. *Nat. Protoc.* **4**, 1064–1072 (2009).
28. L. Wang *et al.*, Notch-dependent repression of miR-155 in the bone marrow niche regulates hematopoiesis in an NF- $\kappa$ B-dependent manner. *Cell Stem Cell* **15**, 51–65 (2014).
29. F. R. Greten *et al.*, IKK $\beta$  links inflammation and tumorigenesis in a mouse model of colitis-associated cancer. *Cell* **118**, 285–296 (2004).
30. B. B. Madison *et al.*, Cis elements of the villin gene control expression in restricted domains of the vertical (crypt) and horizontal (duodenum, cecum) axes of the intestine. *J. Biol. Chem.* **277**, 33275–33283 (2002).
31. A. Oeckinghaus, T. S. Postler, S. Ghosh, Consequences of Nkiras deficiency for the EGF response. NCBI Gene Expression Omnibus (GEO). <https://www.ncbi.nlm.nih.gov/geo/query/acc.cgi?acc=GSE216127>. Deposited 19 October 2022.
32. A. Subramanian *et al.*, Gene set enrichment analysis: A knowledge-based approach for interpreting genome-wide expression profiles. *Proc. Natl. Acad. Sci. U.S.A.* **102**, 15545–15550 (2005).
33. V. K. Mootha *et al.*, PGC-1 $\alpha$ -responsive genes involved in oxidative phosphorylation are coordinately downregulated in human diabetes. *Nat. Genet.* **34**, 267–273 (2003).
34. E. Cerami *et al.*, The cBio cancer genomics portal: An open platform for exploring multidimensional cancer genomics data. *Cancer Discov.* **2**, 401–404 (2012).
35. J. Gao *et al.*, Integrative analysis of complex cancer genomics and clinical profiles using the cBioPortal. *Sci. Signal* **6**, pl1 (2013).
36. M. J. Goldman *et al.*, Visualizing and interpreting cancer genomics data via the Xena platform. *Nat. Biotechnol.* **38**, 675–678 (2020).
37. V. Licursi, F. Conte, G. Fisco, P. Paci, MIENTURNET: An interactive web tool for microRNA-target enrichment and network-based analysis. *BMC Bioinformatics* **20**, 545 (2019).